Cellular Microbiology (2009) **11**(4), 540–550
doi:10.1111/j.1462-5822.2009.01283.x
First published online 16 January 2009

Technoreview

Live cell fluorescence microscopy to study microbial pathogenesis

Adam D. Hoppe,[1]* Stephanie Seveau[2] and Joel A. Swanson[3]

[1]*Department of Chemistry and Biochemistry, South Dakota State University, Brookings, SD 57007-0896, USA.*

[2]*Department of Microbiology and Center for Microbial Interface Biology, Ohio State University Columbus, OH 43210, USA.*

[3]*Department of Microbiology and Immunology, University of Michigan Medical School, Ann Arbor, MI 48109-5620, USA.*

Summary

Advances in microscopy and fluorescent probes provide new insight into the nanometer-scale biochemistry governing the interactions between eukaryotic cells and pathogens. When combined with mathematical modelling, these new technologies hold the promise of qualitative, quantitative and predictive descriptions of these pathways. Using the light microscope to study the spatial and temporal relationships between pathogens, host cells and their respective biochemical machinery requires an appreciation for how fluorescent probes and imaging devices function. This review summarizes how live cell fluorescence microscopy with common instruments can provide quantitative insight into the cellular and molecular functions of hosts and pathogens.

Introduction

In the nineteenth century, Mechnikov took advantage of light microscopy to peer into the worlds of microorganisms and their interactions with phagocytes. By simply watching the behaviour of cells, he discovered that 'cellular eating' or phagocytosis was a fundamental mechanism of immune defence. The optical microscope has undergone tremendous changes since then. New instrumentation and techniques for fluorescence microscopy allow observation of living cells with minimal perturbation of their normal function. While conventional molecular biological, genetic and proteomics approaches are important for identifying and characterizing protein–protein interactions, only microscopy has the potential to determine the organization and dynamics of macromolecules in the context of a living cell. Foremost among the improvements of light microscopy are the development of fluorescent protein technologies for labelling individual proteins and new probes for measuring chemical analytes such as calcium. Fluorescence resonance energy transfer (FRET) of fluorescently tagged proteins has extended the reach of fluorescence microscopes to the macromolecular scale. FRET and ratiometric microscopy allow measurement of the movements of cellular molecules as well as the molecular interactions that organize cell function. These data provide the spatial and dynamic information necessary for building mechanistic mathematical models of the cellular pathways involved in host–pathogen interactions (also see Linderman and Kirschner in this issue).

Pathogenic microbes exert multiple strategies to subvert host cell functions and to modulate immune responses in the host organisms. Understanding the fundamental processes involved in these events requires detailed study of localized and transient molecular events within pathogens and host cells. For example, intracellular bacterial pathogens reach their specific replicative niche by manipulating host molecules to alter the dynamic endocytic pathways. New live cell imaging techniques hold great promise for explaining the events that control bacterial uptake, endocytic traffic and evasion of immune response. The challenges of studying molecular function by fluorescence microscopy are threefold: they require sensitive and specific probes, adequate resolution in time and space, and some measure of how well the image reflects a relevant biological truth. This review summarizes fluorescent probe technologies that are specific for particular biochemical activities and fluorescence imaging techniques that can turn these signals into dynamic images of intracellular biochemistry. We highlight studies

Received 18 November, 2008; revised 23 December, 2008; accepted 29 December, 2008. *For correspondence. E-mail adam.hoppe@sdstate.edu; Tel. (+1) 605 688 5315; Fax (+1) 605 688 6364.

that have successfully applied live cell fluorescence microscopy to questions of host-cell responses to infection, including studies of *Listeria*, *Yersinia*, *Salmonella* and *Mycobacteria* invasion processes. New technologies for imaging host–pathogen interactions in living tissues and in intact animals are described in recent reviews (Piwnica-Worms *et al*., 2004; Yeung *et al*., 2005; Enninga *et al*., 2007; Mansson *et al*., 2007) and in the accompanying article by Miller in this issue.

The uses of fluorescent probes

Fluorescent protein chimeras to follow the dynamics of host proteins

Naturally fluorescent proteins (FP) derived from jellyfish and coral have allowed the development of sensitive, genetically encoded reporters of signal transduction networks and protein dynamics in living cells and whole animals. Molecular biology and directed evolution methods have created a large variety of FPs, many of which have been optimized for spectral features and biochemical properties, such as reduced oligomerization (Shaner *et al*., 2004; Nguyen and Daugherty, 2005), pH-sensitivity (Miesenbock *et al*., 1998) and photoconversion (Patterson and Lippincott-Schwartz, 2002). FP chimeras are often expressed by transient transfection or stable transformation of cells with plasmids, by retrovirus-based expression or by homologous recombination for stable integration of genes encoding FP chimeras (Huh *et al*., 2003). FP chimeras are now available in many spectral varieties with high quantum yields, including cyan fluorescent protein (CFP), yellow fluorescent protein (YFP), green fluorescent protein (GFP), red fluorescent protein (RFP) and Cherry, among others (Shaner *et al*., 2004). Most applications use FP chimeras to infer the distributions of their endogenous unlabelled counterparts. For example, GFP-actin chimeras report the distributions of actin in cells. A large number of research groups now use FP chimeras to analyse the spatial organization of pathways for signalling and organelle trafficking.

As with all fluorescent probes, FP chimeras present some potential disadvantages. First, the presence of the FP in the protein structure can interfere with essential functions of the natural protein, such as interactions that regulate localization or activity. Second, the intracellular behaviours of low-abundance proteins may be difficult to study using FP chimeras as these chimeras may be present at concentrations approaching single molecules, a situation for which GFP is usually not sufficiently bright relative to cellular autofluorescence. This difficulty is often compensated for by expression of high levels of FP chimera, which may create misleading distributions in cells. Third, overexpression of FP chimera can interfere with endogenous signalling pathways, by creating unusual conditions for regulatory proteins or target molecules. Therefore, the tremendous experimental advantages afforded by FP chimeras must be exploited with appropriate concern for the potential distortions caused by the probes. For each new FP chimera, it is important to characterize the extent to which it reports signals and perturbs pathways, although accurate methods for this are often hard to come by.

Fluorescent protein chimeras have been used in live cell microscopy to follow many host–pathogen interactions. Live cell imaging implicated two members of the Ras superfamily of low molecular weight GTPases, Rab22a and Rab14, in phagosomal arrest induced by *Mycobacterium tuberculosis* var. *bovis* (BCG) in macrophages. BCG utilizes different strategies to arrest vacuolar maturation at the early endosomal stage, thereby avoiding phagosome–lysosome fusion and creating a vacuolar compartment where bacteria survive and proliferate. FP chimeras of Rab22a and Rab14 (GFP-Rab22a, EGFP-Rab14) persisted on BCG-containing phagosomes, whereas the GFP-Rab5 and GFP-Rab21 were only transiently recruited. Furthermore, Rab22a and Rab14 activities were required to prevent the acquisition of Rab7 and successive fusion with lysosomes (Kyei *et al*., 2006; Roberts *et al*., 2006). In these experiments, GFP-chimera recruitment to phagosomes was measured from three-dimensional (3D) reconstructions of confocal fluorescence microscope images collected at many planes of focus.

Salmonella enterica serovar Typhimurium proliferates in *Salmonella*-containing vacuoles (SCVs) inside macrophages and epithelial cells. After SCVs form, they acquire some but not all markers of late endosomes and lysosomes (Meresse *et al*., 1999). To control its intracellular fate, *Salmonella* utilizes type III secretion systems (T3SS), which inject protein effectors across the SCV membrane to actively manipulate the host cell chemistry. The T3SS is required for the formation of highly dynamic tubular membrane structures, called *Salmonella*-induced filaments (SIFs), which originate from the host cell endosomal system within hours after infection. The biogenesis and dynamics of SIFs were followed by live cell imaging in epithelial cells using the lysosomal marker LAMP1-GFP and endocytosed fluorescent dextran. SIFs are unique morphological alterations of endosomes which move and extend along microtubules and are transiently connected with the SCVs (Drecktrah *et al*., 2008; Rajashekar *et al*., 2008). The SCV is connected to the endocytic pathway, a feature that may be crucial for addition of membranes for the extension of the vacuole and for bringing nutrients to the bacteria (Drecktrah *et al*., 2007).

Entry of *Listeria monocytogenes* into non-phagocytic cells utilizes cholesterol-enriched membrane microdomains and clathrin- and dynamin-dependent inter-

nalization processes (Seveau *et al*., 2004; Veiga *et al*., 2007). The assembly and disassembly of clathrin and dynamin structures at the forming vacuole containing *L. monocytogenes* was detected by live cell imaging of the clathrin-GFP, and dynamin2-mRFP associated with the vacuole (Veiga *et al*., 2007). Although the duration of bacterial uptake ($\geq$ 2 min) and the size of the vacuoles (1–2 μm) are significantly different from those of the classical clathrin-mediated endocytic events (0.5–3 min and ~0.1 μm), these results demonstrated that lipid raft-, clathrin- and dynamin-mediated internalization routes, which are normally utilized by host cells during receptor-mediated endocytosis, are subverted by the bacteria to access the intracellular compartment of non-phagocytic cells.

The successive steps of the biogenesis of *L. monocytogenes*-containing vacuoles and bacterial escape from the vacuole were determined by widefield fluorescence microscopy of macrophages expressing FP chimeras. These studies measured the recruitment over time of FP chimeras of endocytic markers, the loss of fluid-phase fluorescent markers ingested together with the bacteria, and the permeation of vacuoles by a YFP-labelled cell wall-binding domain (YFP-CBD) of the *Listeria* phage endolysin Ply118, as an indicator of bacterial escape (Loessner *et al*., 2002; Henry *et al*., 2006). These studies demonstrated that *L. monocytogenes* are internalized within compartments that rapidly mature into late endosomes (labelled with YFP-Rab7), from which they escape after 15–30 min, avoiding vacuolar fusion with lysosomal compartments (labelled with LAMP1-CFP) (Henry *et al*., 2006). Listeriolysin O (LLO), the cytolysin secreted by *L. monocytogenes*, plays a key role in escape. Live cell imaging allowed identification of the compartment and timing of the escape process. A LLO-deficient bacterial strain localized within phagosomes that acquired the late endosomal and lysosomal marker LAMP1-CFP at a higher rate in comparison to the wild-type strain, and remained trapped in a degradative compartment characterized by the accumulation of LAMP1-CFP.

Fluorescent probes that measure ions

Methods to study molecular mechanisms of pathogenesis in living cells employ a variety of fluorescent reporters of molecular processes in living cells. Fluorescent dyes can measure intracellular ions, such as pH and intracellular free calcium ([Ca^{++}_{free}]) (O'Connor and Silver, 2007). These methods require sensitive detection technologies and an appreciation for how the probes may misrepresent or interfere with the processes they are intended to measure. Probes of [Ca^{++}_{free}] provide a case in point. A fluorescent probe of [Ca^{++}_{free}] must be delivered into the cytosolic space without significantly damaging the plasma membrane or labelling other compartments. [Ca^{++}_{free}] is normally less than 0.1 μM in unstimulated cells, and fluorescent probe concentration and affinity for [Ca^{++}_{free}] must be such that they report physiologically relevant increases in calcium without buffering calcium. Calcium indicators must be sufficiently bright in both the bound and unbound states that they can be detected at low intracellular probe concentrations. Weakly fluorescent probes (such as the early generation probe quin2) must be measured at such high concentrations that they buffer intracellular calcium, dampen signals and cause toxicity. On the other hand, small, soluble, calcium indicators with high affinity for calcium can also misrepresent subcellular localization of [Ca^{++}_{free}] changes, as they may diffuse some distance from their sites of calcium-binding before losing bound calcium and changing their fluorescence (Demuro and Parker, 2006). The present generation of fluorescent calcium indicators is highly developed in these regards, and there is now a variety of commercially available, robust and sensitive probes of [Ca^{++}_{free}] for different applications (Simpson, 2006).

The environment of the probe can alter its responses to analytes. The affinities of the probes for calcium decrease below pH 6.8. Thus, probes that reliably report [Ca^{++}_{free}] in cytoplasm (pH 6.8–7.0) have lower affinities for calcium in acidic vacuolar compartments. Measurements of calcium in lysosomes and acidic organelles could be obtained by coordinated measurements of pH and calcium (Christensen *et al*., 2002). This method allowed measurements of vacuolar pH and calcium concentrations during escape of *Listeria monocytogenes* from vacuoles in macrophages. Those studies indicated that LLO in *Listeria*-containing vacuoles increases pH and depletes calcium shortly after bacterial entry (Shaughnessy *et al*., 2006). These alterations of transmembrane ion gradients may slow vacuole fusion with lysosomes.

Salmonella responds to the environment inside the SCV of host cells by changes in gene expression. The two-component regulatory system PhoP-PhoQ responds *in vitro* to low pH and low Mg^{++} concentrations. Early studies using fluorescein-labelled dextran to measure SCV pH showed that *Salmonella* delay SCV acidification, relative to rates seen in pinosomes and phagosomes, but require acidification for activation of PhoP-activated genes (Alpuche-Aranda *et al*., 1992). Later studies demonstrated that decreases in Mg^{++} regulated the PhoP-PhoQ system *in vitro* (Garcia Vescovi *et al*., 1996), and indicated that this was the principal regulatory ion activating PhoP *in vivo*. However, Martin-Orozco *et al*. (2006) used microscopy of novel fluorescent reporters of Mg^{++} called PEBBLES to measure conditions in the SCV and found that Mg^{++} concentrations were not in a range that would affect the PhoP-PhoQ regulon. These findings

highlight the importance of measuring analyte concentrations in the context of the living cell.

Microscopy methods

For microscopy to explain the molecular mechanisms of host–pathogen interactions, it should determine the localization, activities and interactions of all of the relevant molecules. Accordingly, an 'ideal microscope' would record this information for the proteins of the host cell and the pathogen at nanometer spatial resolution and microsecond temporal resolution. Furthermore, this measurement should not perturb the biological system. If this were possible, the scientist's job would simply be to record and interpret images. In reality, current microscopes can image no more than about five FP-tagged molecules simultaneously in a live cell with millisecond and ~200–500 nm resolution. The researcher is therefore left to study a small sample of intracellular biochemistry while balancing efforts to maximize sensitivity, resolution and to minimize perturbation of the biological system.

We expect images acquired from a microscope to map the relative locations and concentrations of molecules inside the cell. However, fluorescence images carry distortions that limit resolution and alter the correspondence between probe concentration and image intensity. These distortions arise from the fact that the structures being imaged are of the same size as the wavelength of light used to image them. The result is a blurring of boundaries of small objects, which limits the microscope's ability to resolve them. Additionally, this blurring has the subtle effect of averaging fluorescence between adjacent volume elements. This problem is so pervasive in microscopy that essentially all measurements of subcellular biochemistry are influenced by blurring.

Many labs have access to three imaging modalities: widefield (standard fluorescence microscope), confocal and total internal reflection fluorescence (TIRF) microscopes. Each of these microscopes imparts different kinds of distortion on the data, which can be characterized by the point spread function (PSF). The PSF is a 3D image of the fluorescence emanating from an infinitely small point. A PSF can be used to describe the performance of the imaging system and to reverse the blurring distortion using computational methods such as iterative deconvolution (Agard and Sedat, 1983; Verveer and Jovin, 1997; Holmes *et al*., 2006). For more detailed descriptions about how each microscope works, the reader is referred to The Handbook of Confocal Microscopy (Pawley, 2006). For the purposes of this review, we simply compare the potential of these instruments for imaging host–pathogen interactions at the cellular level.

Common modes of detection

Widefield microscopes create a uniform field of excitation light. Fluorescence emitted from the sample is then imaged directly onto a camera. The resulting image is relatively sharp in the *x*-*y* plane (the image one normally sees when looking through the eyepiece) but is significantly blurred along the *z*-axis. This distortion can be seen in the PSF (Fig. 1A) which has a finite diameter of about 200 nm in the in-focus *x*-*y* plane but extends infinitely along the *z*-axis. The impact of this PSF on the data can be seen in the blurred image in Fig. 1A.

Confocal fluorescence microscopes illuminate the sample with light focused to a point through a pinhole (or an array of pinholes). A conjugate pinhole in the imaging plane (or an array of pinholes) rejects out-of-focus fluorescence. The resulting PSF is smaller than that from the widefield microscope (Fig. 1B). Although it is still elongated along the *z*-axis, it has a finite boundary (unlike the PSF for the widefield microscope). This property makes the confocal microscope particularly well suited for imaging in thick specimens.

The TIRF microscope takes advantage of the refractive index difference between coverslips and cell culture media. TIRF illumination creates a shallow illumination field that decays exponentially away from the coverslip–medium interface. This property allows selective imaging of molecules within ~100–200 nm of a coverslip. By excluding fluorophores in other focal planes, TIRF allows fluorescence imaging with very low background fluorescence. This feature makes TIRF microscopy the predominant mode for imaging single fluorescent molecules attached to glass surfaces or inside adherent cells (Ha *et al*., 1996; Cai *et al*., 2007). The PSF for the TIRF microscope is similar to the widefield microscope; however, the high numerical apertures used for TIRF objectives (NA = 1.49) and the close proximity of fluorescence to the coverslip make this PSF somewhat smaller than the widefield and confocal PSFs encountered in lower numerical aperture water immersion objectives (NA = 1.2) used for live cell imaging.

Each of these microscopes has strengths and weaknesses for live cell imaging that depend on their speed, resolution and sensitivity. The widefield microscope has the lowest 3D resolution, but is relatively inexpensive. Additionally, widefield microscopes equipped with filter wheels for selection of excitation and emission wavelengths have proven to be sufficiently fast for ratiometric and FRET based analysis in live cells. For 3D imaging of multiple colours and FRET analysis, more sophisticated configurations are needed to acquire data at rates faster than cellular movements (e.g. complete acquisition of the 3D data set in approximately 1 s). Recently, we devised a widefield microscope that used multiple cameras, fast

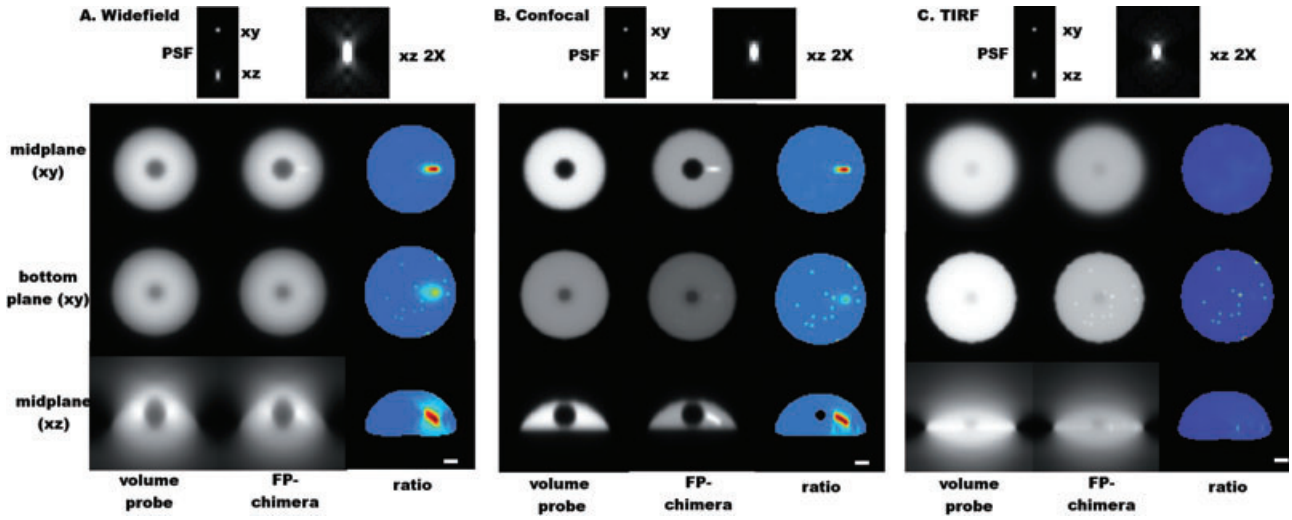

Fig. 1. Imaging host–pathogen interactions in widefield, confocal and TIRF microscopy. A computer-generated model of a host cell was 'infected' *in silico* with an intracellular bacterium (1.5 × 0.3 μm rod to the right of the nucleus, most easily seen in the confocal image) and multiple viruses located on the bottom membrane (100 nm in diameter). Two FP-chimeras were simulated, one that is free in the cytosol of the host cell (left panel) and one that is also present in the cytosol and recruited to the bacterium and virions (recruitment doubles the local concentration of this FP). To simulate imaging with various microscopes, a uniform illumination field was applied for widefield and confocal imaging and an exponentially decaying field was applied for TIRF (characteristic distance of 100 nm). The images were then blurred with the PSF for each microscope (top row). A 2× magnification of the *x-z* slice of the PSF is displayed with enhanced contrast to illustrate the differences between microscopes. Three slices are shown, an *x-y* image in the middle of the cell (along *z*), an image at the bottom membrane and an *x-z* image taken from the middle of the y direction.
A. Widefield images are significantly blurred; however, ratiometric microscopy still recovers the relative distributions of the two probes as seen by the appearance of virions and the bacterium.
B. Confocal images are significantly sharper due to a smaller and more well-defined PSF. The sharpness of the raw data translates into improvements in the ratio image as well.
C. Lastly, TIRF images show the bottom membrane clearly but other *z*-planes only contain out-of-focus light. Here the virions on the bottom of the cell are clearly visible and the ratio image is very sharp; however, the intracellular bacterium cannot be observed.
Scale bar is 1 μm. PSFs were simulated for 1.2 NA, water-immersion objective for the widefield and confocal and a 1.49 NA objective for TIRF.

hardware coordination and image reconstruction to achieve sustained multicolour and FRET of living cells in three dimensions (Hoppe *et al.*, 2008). The confocal microscope has improved resolution over widefield microscopes, but image acquisition can be slow, and much fluorescence is discarded in making an image. This can lead to considerable photobleaching of specimens. The speed limitations have been improved by the development of spinning disc and array-scan microscopes (Pawley, 2006). Additionally, 3D imaging with a confocal microscope requires acquisition of more focal sections than a widefield microscope. Lastly, TIRF microscopy offers the best *z*-axis resolution and exquisite sensitivity, but is limited to imaging fluorophores near coverslips. For example, the bacterium in Fig. 1 does not contact the bottom membrane of the cell and is therefore not observed in the TIRF image. In all cases, the speed and duration of imaging that can be performed in live cells is limited by the stability of the fluorophores and the toxicity generated by the excitation light and the fluorophores themselves.

While imaging an individual FP-chimera with these microscopes is instructive, simultaneous analysis of multiple FP-chimeras tell a deeper story. Three questions can be addressed by using these microscopes to image multiple fluorophores during a cellular process: (i) how similar are the distributions of two probes (ii) how do their localizations change in response to interactions with microbes and (iii) how do the molecular interactions between two labelled proteins change? These questions are addressed by colocalization and image correlation microscopies, ratiometric fluorescence microscopy and FRET microscopy.

Colocalization

Colocalization, or the comparison of the distributions of two fluorescent probes, is particularly useful for defining the intracellular compartment in which a particular protein is located. Colocalization studies are routinely used to analyse the trafficking of intracellular microbes, as in the examples described above for *Mycobacteria*, *Listeria* and *Salmonella*. The typical approach for colocalization is to collect one image for each probe and then to compare their patterns by means of overlaying them. Typically, the image of one probe is coloured green and the image of

the other probe is coloured red. When these images are overlayed, subcellular regions occupied by both probes appear yellow. For probes that show nearly identical subcellular distributions, their perfect colocalization can be strong evidence that they belong to the same subcellular compartment. For such measurements to be valid, the microscope must cleanly distinguish the two probes as spectral cross-over between probe channels can lead to erroneous colocalization.

Ambiguity also arises in this approach when the probes show only partial colocalization. For example, if one probe is distributed throughout the cell (e.g. endoplasmic reticulum), then occasional overlapping fluorescence from the other probe cannot be taken to indicate colocalization. All too often, the interpretation becomes subjective and the researcher must consider the likelihood that the low frequency of colocalization is caused by a biological mechanism rather than chance. To answer this question with greater accuracy, new approaches are being developed for quantitative colocalization, including image cross-correlation methods and the Manders coefficients (Comeau *et al.*, 2006; Oheim and Dongdong, 2007). Effectively, these methods quantify how often and in how many pixels two different probes are present. Such methods are particularly useful for comparing changes in colocalization (say before and after treatment with a drug) of a particular probe-pair, but are generally underused.

While colocalization indicates similar distributions to subcellular structures, it cannot be used to demonstrate direct molecular interactions. This limitation arises from the fact that the microscope's resolution limit of ~200 nm is much larger than the dimensions of molecular interactions (Fig. 2). Hence, probes can accumulate independently on a subcellular structure and report fluorescence from the same unresolvable point despite significant spatial separation. Additionally, intense accumulation of probes to different structures, but weak colocalization, may mask subtle but important interactions. The development of super-resolution methods such as photo-activated localization microscopy (PALM) (Betzig *et al.*, 2006) and stochastic optical reconstruction microscopy (STORM) (Rust *et al.*, 2006) can push the resolution of the optical microscope down to ~10 nm. As these methods approach molecular resolution, colocalization signals can become indicative of molecular interactions.

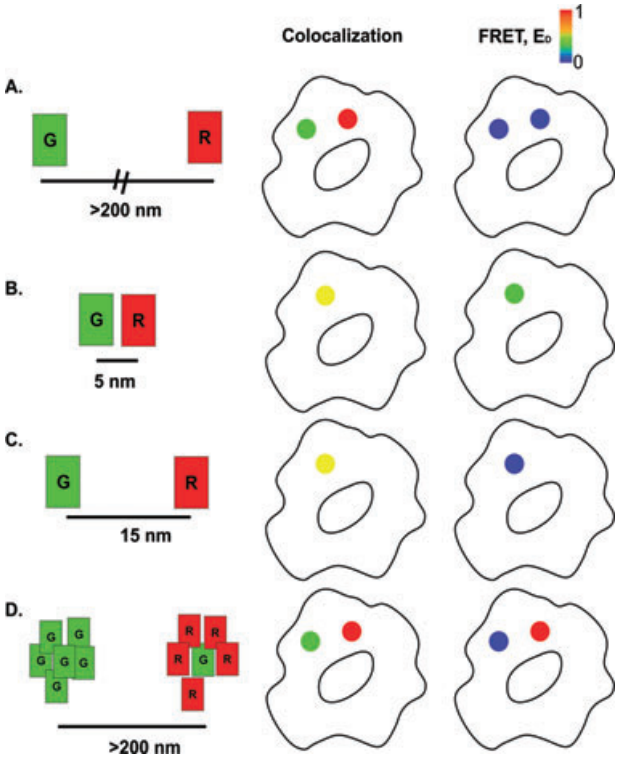

Fig. 2. Comparison of colocalization and FRET Imaging.
A. Green and Red probes separated by a distance greater than the resolving power of the optical microscope (at least 200 nm) show distinct localizations (red and green spots).
B. Probes that interact directly, however, will be below the resolution limit of the microscope and appear colocalized (yellow spot). Additionally, if they are close enough together (less than about 8 nm), they can undergo FRET, which is strong evidence for a direct interaction. (FRET is shown here as E_D which ranges from 0 to 1 and is proportional to the fraction of bound green probes and the FRET efficiency).
C. Probes that localize to subdiffraction limit-sized structures can appear colocalized, even though they do not interact directly. FRET will not be observed in this structure (provided the probe densities are sufficiently low).
D. Skewed stoichiometry can create situations in which two molecules appear to not colocalize; however, saturating amounts of acceptor lead to high FRET signals from the donor.

Ratiometric microscopy

A more quantitative variation on colocalization is ratiometric fluorescence microscopy. Here, the localization dynamics of a labelled fluorescent protein are recorded relative to another fluorescent molecule that marks cytoplasmic volume or cell membranes. For example, in an image in which the FP-chimera is localized to the cytosol, a ratio with a volume-marking fluorophore creates a uniform image. However, if the FP-chimera localizes to a subcellular region, the ratio of FP-chimera/FP-volume in that region will increase. This technique distinguishes changes in the distribution of FP-chimeras from changes in cell shape and the movement of probe-displacing organelles. A simulation illustrates the utility of ratiometric imaging for discerning small changes in probe localization (Fig. 1). The widefield microscope is capable of detecting weak signals from virions inside a cell and the confocal microscope and TIRF microscope are better at detecting these localized signals due to their improved 3D sectioning capabilities. In addition to blurring, detection noise also affects the quality of the ratio image. For live cell

imaging in the confocal microscope, the improved *z*-axis resolution is somewhat offset by increased noise relative to the widefield microscope.

FRET microscopy for detection of molecular interactions

Fluorescence resonance energy transfer is an established and powerful method to quantify formation and dissociation of protein complexes (Sekar and Periasamy, 2003), the conformational states of individual doubly tagged proteins and the densities of membrane proteins in intact cells. FRET detects interactions between proteins of interest conjugated to appropriate FP by the transfer of energy from an excited donor FP to an acceptor FP in close proximity ($\leq$ 10 nm). This technique provides the spatial and temporal localization of protein interactions with nanometer-scale resolution. Another unique benefit of FP-based FRET techniques is that formation and dissociation of protein pairs can be monitored in real time, as these interactions bring the FPs within the Förster distance (~5 nm). This property distinguishes FRET from techniques that detect protein interactions based on complementation of FPs or light-emitting enzymes (Hu and Kerppola, 2003; Luker *et al*., 2004), as these methods require significant lag times (seconds-hours) for detection and, in the case of FPs, leads to the irreversible formation of fluorescent complexes when the two halves of the FP meld together. Currently, FRET is the only technique capable of probing dynamic interactions and conformational changes with spatial resolution limited by the optics of the microscope.

Numerous methods have been developed for FRET-based analysis of molecular interactions and conformational states (Jares-Erijman and Jovin, 2003). In its simplest form, FRET can be used to detect changes in conformational states of protein domains, when donor and acceptor FPs are attached to either end of these domains. In this case, a simple ratio of acceptor fluorescence to donor fluorescence, during preferential illumination of the donor, is sufficient to detect changes in the FRET efficiency (i.e. the fraction of energy transferred from the donor to the acceptor) as the changes in conformation change the distance between donor and acceptor. When examining the binding of two separate FP-labelled proteins by FRET, more sophisticated methods are needed. Here, the goal can be to obtain qualitative measures that simply detect the presence or absence of an interaction by detecting the FRET-induced acceptor fluorescence (also known as sensitized emission) from a background of overlapping non-FRET fluorescence from the donor and acceptor.

FRET microscopic studies of Rac signalling analysed the effects of the *Yersinia pseudotuberculosis* invasion proteins YopE and YopT on Rac1 activation dynamics (Wong and Isberg, 2005). YopE and YopT are delivered into the cytoplasm of host cells via a T3SS, where they interfere with signalling via the Rho-family GTPases Rac1 and RhoA (Viboud and Bliska, 2005). To examine the effects of YopE and YopT on the localization and activation of Rac1, Cos1 cells were transfected with plasmids encoding CFP-labelled Rac1 and YFP-labelled p21-binding domain (PBD) of Pak1 which binds to active, GTP-bound Rac1 but not to inactive, GDP-bound Rac1. In its active GTP-bound state, Rac1 forms a bimolecular complex with PBD. The proximity of FPs within the YFP-Rac1/CFP-PBD complex allowed FRET detection of YFP-Rac1 activation. The YFP-Rac1 fluorescence indicated the distributions of GTPase and the calculated FRET signals indicated the distributions of the active YFP-Rac1. Using mutant strains of bacteria expressing YopE, YopT or both, Wong and Isberg (2005) determined that the two proteins exerted distinct and counteracting effects on Rac1 activation and distributions. YopE inactivated Rac1 by acting as a GTPase-activating protein (GAP) on plasma membrane-associated Rac1. YopT protease activity released Rac1 from plasma membranes, which led to accumulation of active YFP-Rac1 in the nucleus. When the two Yops were overexpressed in the same cell, the YopT activity led to accumulation of active YFP-Rac1 in the nucleus and the YopE activity inactivated those cytoplasmic YFP-Rac1 molecules which could still associate with the plasma membrane. These distinct effects on Rac1 localization and activation indicated that YopE and YopT can exert complex effects on the spatial organization of Rac1 activity in target cells.

While the methods used in these studies provide relatively simple detection of protein interactions, the measurements do not return the concentrations of interacting FPs or the FRET efficiency, and they cannot be compared between instruments, which precludes full characterization of intracellular biochemical activities. Additionally, all FRET measurements between two ectopically expressed proteins are influenced by the relative expression levels of donor and acceptor FP chimeras. These limitations can be overcome by quantitative FRET methods. Quantitative FRET microscopy seeks to estimate the concentrations of interacting proteins and the distance between FPs, which is described by the FRET efficiency. While currently no methods exist that can quantify all of these aspects in a single, rapid measurement, a number of techniques have been developed to quantify the relative concentrations and apparent FRET efficiencies of the interacting proteins from calibrating the FRET-induced changes in the fluorescence spectrum (Erickson *et al*., 2001; Hoppe *et al*., 2002). Here, the apparent efficiency quantifies the interaction as the fraction of interacting proteins multiplied by the FRET efficiency (Erickson *et al*., 2001). These techniques do not

provide the absolute concentrations of interacting fluorophores, but they do provide a quantitative gauge of the magnitude of an interaction by being proportional to the number of molecules in complex. The use of apparent efficiency is a limitation that arises from the amount of information available in the fluorescence spectrum (Hoppe *et al*., 2002). Importantly, these apparent efficiency measurements are transferable from one instrument to the next and have been extended to fluorescence polarization (Mattheyses *et al*., 2004), and acceptor photobleaching (Jares-Erijman and Jovin, 2003).

FRET-microscopy-based studies were applied to determine the spatio-temporal activation of Rac1 and phosphatidylinositol 3-kinase (PI3K), upon cellular stimulation by the *L. monocytogenes* invasion factor InlB. In cells cotransfected with plasmids encoding YFP-Rac1 and CFP-PBD, these experiments determined the ratio of GTP-bound YFP-Rac1 molecules to the total YFP-Rac1 ([YFP-Rac1GTP/CFP-PBD]/[total YFP-Rac1]). FRET microscopy was also used to measure the density of 3′ phosphoinositides in the plasma membrane, such as phosphatidylinositol (3,4,5)-trisphosphate (PIP3). The quantification of FRET between two co-expressed FP chimeras of the Akt pleckstrin homology domain that specifically associate with 3′ phosphoinositides, YFP-AktPH and CFP-AktPH, was used as read-out of PI3K activity. At low concentrations of InlB, PIP3 was not generated on membranes, the FP chimeras were dispersed in the cytosol and did not exhibit FRET. Upon receptor-mediated activation of PI3K and generation of PIP3, the concentration of the fluorescent AktPH chimeras increased at the plasma membrane, consequently leading to an increase in the FRET signal. These methods showed that upon receptor stimulation by InlB, Rac1 was activated downstream from PI3K within 1 min and was downregulated within 5 min, whereas PIP3 reached its maximum concentration after 3 min and slowly decreased for more than 20 min. The results led to the hypothesis that the spatial distribution of 3′ phosphoinositides within cholesterol-enriched membrane microdomains is critical for the successive activation of Rac1 and consequently for F-actin assembly at bacterial entry site (Seveau *et al*., 2007).

In the analysis of cellular signalling pathways, the ultimate goal of FRET microscopy is to convert fluorescence signals from FP chimeras into concentrations of bound and free proteins and the FRET efficiencies between those interacting proteins. Recovering this information would allow FRET microscopy to measure the exact quantities of interacting components in genetic model systems in which the FP chimeras are expressed from endogenous genetic loci. Additionally, precise concentration estimates would allow new insight into how multisubunit complexes are assembled inside cells by allowing measurement of their stoichiometry during assembly.

Two technical limitations prevent FRET microscopy from reaching its potential for analysis of subcellular pathways. First, with two exceptions (He *et al*., 2003; Galperin *et al*., 2004), FRET microscopy has only been applied to the analysis of interactions between two labelled proteins. This limitation prevents placement of specific interactions into the temporal and spatial context of other biochemical activities, thereby limiting the potential of FRET for constructing models of pathway organization. Multispectral microscopy platforms have the ability to unmix overlapping fluorescence signals and thus to allow observation of multiple fluorescently tagged molecules (Neher and Neher, 2004; Nadrigny *et al*., 2006). However, these methods are not currently capable of measuring FRET between multiple fluorophores and therefore are limited to measuring the colocalization of fluorescently tagged molecules. Second, FRET microscopy measurements are significantly impaired by out-of-focus light and detection noise (Hoppe *et al*., 2008). These limitations lead to reduced sensitivity and accuracy in FRET measurements and limit live cell 3D-FRET microscopy. Until these limitations are overcome, the potential of FRET microscopy for measuring the timing and spatial organization of biochemical reactions inside cells will not be realized.

Advanced techniques

New developments in microscopes and image processing techniques are extending the capabilities of live cell fluorescence microscopy. Recently, methods were developed for fast imaging of molecular interactions throughout the 3D-space of the living cell (Hoppe *et al*., 2008). This work included the development of new instrumentation and new algorithms for the deblurring of 3D-FRET microscopy data to achieve sustained imaging of the activation of Cdc42 during FcR-mediated phagocytosis of beads. Additionally, new advances in super-resolution microscopy hold the promise of improving protein localization and FRET measurements. While many of these super-resolution techniques require extravagant instrumentation, some, such as PALM, STORM and structured illumination microscopy (SIM)(Schermelleh *et al*., 2008) have the potential to see immediate application to host–pathogen problems. PALM and STORM are exciting developments because they allow imaging of photoactivatable proteins in thin sections of fixed cells with 2D-resolution similar to the scale of single protein interactions (2–25 nm range) (Betzig *et al*., 2006). PALM has also been applied to live cell microscopy with TIRF illumination, but in this configuration it is limited to the analysis of slow moving membrane-associated structures and has reduced resolution over fixed-cell PALM (~60 nm) (Shroff *et al*., 2008). Recently developed 3D-SIM methods provide a new level of resolution for imaging of

the 3D architecture of cells. By patterning excitation light in 3D and then collecting images for various orientations of these patterns, 3D-SIM improves the 3D resolution of the optical microscope to ~100 nm × 100 nm × 300 nm, a twofold resolution improvement over the confocal microscope (Gustafsson *et al*., 2008; Schermelleh *et al*., 2008). In addition to improving the resolution of the microscope, this technique holds the possibilities of being performed on live cells and providing quantitative analysis of colocalization, ratiometric imaging and FRET microscopy. This exciting possibility may lead to new views of the dynamic chemistries that control cell function.

New intravital imaging techniques are bridging the gap between high-resolution analysis of host–pathogen interactions in cultured cells with their analysis inside living animals. Techniques such as single-plane illumination microscopy (Huisken *et al*., 2004) and scanned sheet microscopy (Keller *et al*., 2008), in addition to multiphoton microscopy (Miller, this issue), provide new tools for imaging host–pathogen interactions in tissue.

Conclusion

Numerous key effectors that participate in host cell subversion by pathogens have been identified and many more will be identified. A major challenge is to determine how these effectors are assembled and coordinate their activities in time and space during invasive processes. Quantitative imaging methods that follow several kinds of molecule in living cells will facilitate discovery of dynamic and sequential interactions as well as subcellular localization. In turn, mechanistic mathematical modelling (Linderman and Kirshner, this issue) of these data will provide new levels of description of the molecular pathways that control host–pathogen interactions.

Acknowledgements

This study was supported by NIH grants AI-035950 and AI-064668 (to J.A.S.).

References

Agard, D.A., and Sedat, J.W. (1983) Three-dimensional architecture of a polytene nucleus. *Nature* **302:** 676–681.

Alpuche-Aranda, C.M., Swanson, J.A., Loomis, W.P., and Miller, S.I. (1992) *Salmonella typhimurium* activates virulence gene transcription within acidified phagosomes. *Proc Nat Acad Sci USA* **89:** 10079–10083.

Betzig, E., Patterson, G.H., Sougrat, R., Lindwasser, O.W., Olenych, S., Bonifacino, J.S., *et al.* (2006) Imaging intracellular fluorescent proteins at nanometer resolution. *Science* **313:** 1642–1645.

Cai, D., Verhey, K.J., and Meyhofer, E. (2007) Tracking single Kinesin molecules in the cytoplasm of mammalian cells. *Biophys J* **92:** 4137–4144.

Christensen, K.A., Myers, J.T., and Swanson, J.A. (2002) pH-dependent regulation of lysosomal calcium in macrophages. *J Cell Sci* **115:** 599–607.

Comeau, J.W., Costantino, S., and Wiseman, P.W. (2006) A guide to accurate fluorescence microscopy colocalization measurements. *Biophys J* **91:** 4611–4622.

Demuro, A., and Parker, I. (2006) Imaging single-channel calcium microdomains. *Cell Calcium* **40:** 413–422.

Drecktrah, D., Knodler, L.A., Howe, D., and Steele-Mortimer, O. (2007) *Salmonella* trafficking is defined by continuous dynamic interactions with the endolysosomal system. *Traffic* **8:** 212–225.

Drecktrah, D., Levine-Wilkinson, S., Dam, T., Winfree, S., Knodler, L.A., Schroer, T.A., and Steele-Mortimer, O. (2008) Dynamic behavior of *Salmonella*-induced membrane tubules in epithelial cells. *Traffic* **9:** 2117–2129.

Enninga, J., Sansonetti, P., and Tournebize, R. (2007) Roundtrip explorations of bacterial infection: from single cells to the entire host and back. *Trends Microbiol* **15:** 483–490.

Erickson, M.G., Alseikhan, B.A., Peterson, B.Z., and Yue, D.T. (2001) Preassociation of calmodulin with voltage-gated Ca(2+) channels revealed by FRET in single living cells. *Neuron* **31:** 973–985.

Galperin, E., Verkhusha, V.V., and Sorkin, A. (2004) Three-chromophore FRET microscopy to analyze multiprotein interactions in living cells. *Nat Methods* **1:** 209–217.

Garcia Vescovi, E., Soncini, F.C., and Groisman, E.A. (1996) Mg2+ as an extracellular signal: environmental regulation of *Salmonella* virulence. *Cell* **84:** 165–174.

Gustafsson, M.G., Shao, L., Carlton, P.M., Wang, C.J., Golubovskaya, I.N., Cande, W.Z., *et al.* (2008) Three-dimensional resolution doubling in wide-field fluorescence microscopy by structured illumination. *Biophys J* **94:** 4957–4970.

Ha, T., Enderle, T., Ogletree, D.F., Chemla, D.S., Selvin, P.R., and Weiss, S. (1996) Probing the interaction between two single molecules: fluorescence resonance energy transfer between a single donor and a single acceptor. *Proc Natl Acad Sci USA* **93:** 6264–6268.

He, L., Olson, D.P., Wu, X., Karpova, T.S., McNally, J.G., and Lipsky, P.E. (2003) A flow cytometric method to detect protein–protein interaction in living cells by directly visualizing donor fluorophore quenching during CFP→YFP fluorescence resonance energy transfer (FRET). *Cytometry A* **55:** 71–85.

Henry, R., Shaughnessy, L., Loessner, M.J., Alberti-Segui, C., Higgins, D.E., and Swanson, J.A. (2006) Cytolysin-dependent delay of vacuole maturation in macrophages infected with *Listeria monocytogenes*. *Cell Microbiol* **8:** 107–119.

Holmes, T.J., Briggs, D., and Abu Tarif, A. (2006) Blind deconvolution. In *Handbook of Biological Confocal Microscopy*. Pawley, J.B. (ed.). New York: Springer, pp. 468–487.

Hoppe, A., Christensen, K., and Swanson, J.A. (2002) Fluorescence resonance energy transfer-based stoichiometry in living cells. *Biophys J* **83:** 3652–3664.

Hoppe, A.D., Shorte, S.L., Swanson, J.A., and Heintzmann, R. (2008) Three-dimensional FRET reconstruction micro-

scopy for analysis of dynamic molecular interactions in live cells. *Biophys J* **95:** 400–418.

Hu, C., and Kerppola, T. (2003) Simultaneous visualization of multiple protein interactions in living cells using multicolor fluorescence complementation analysis. *Nat Biotechnol* **21:** 539–545.

Huh, W.K., Falvo, J.V., Gerke, L.C., Carroll, A.S., Howson, R.W., Weissman, J.S., and O'Shea, E.K. (2003) Global analysis of protein localization in budding yeast. *Nature* **425:** 686–691.

Huisken, J., Swoger, J., Del Bene, F., Wittbrodt, J., and Stelzer, E.H. (2004) Optical sectioning deep inside live embryos by selective plane illumination microscopy. *Science* **305:** 1007–1009.

Jares-Erijman, E.A., and Jovin, T.M. (2003) FRET imaging. *Nat Biotechnol* **21:** 1387–1395.

Keller, P.J., Schmidt, A.D., Wittbrodt, J., and Stelzer, E.H. (2008) Reconstruction of zebrafish early embryonic development by scanned light sheet microscopy. *Science* **322:** 1065–1069.

Kyei, G.B., Vergne, I., Chua, J., Roberts, E., Harris, J., Junutula, J.R., and Deretic, V. (2006) Rab14 is critical for maintenance of *Mycobacterium tuberculosis* phagosome maturation arrest. *EMBO J* **25:** 5250–5259.

Loessner, M.J., Kramer, K., Ebel, F., and Scherer, S. (2002) C-terminal domains of *Listeria monocytogenes* bacteriophage murein hydrolases determine specific recognition and high-affinity binding to bacterial cell wall carbohydrates. *Mol Microbiol* **44:** 335–349.

Luker, K.E., Smith, M.C., Luker, G.D., Gammon, S.T., Piwnica-Worms, H., and Piwnica-Worms, D. (2004) Kinetics of regulated protein–protein interactions revealed with firefly luciferase complementation imaging in cells and living animals. *Proc Natl Acad Sci USA* **101:** 12288–12293.

Mansson, L.E., Melican, K., Molitoris, B.A., and Richter-Dahlfors, A. (2007) Progression of bacterial infections studied in real time – novel perspectives provided by multiphoton microscopy. *Cell Microbiol* **9:** 2334–2343.

Martin-Orozco, N., Touret, N., Zaharik, M.L., Park, E., Kopelman, R., Miller, S., *et al.* (2006) Visualization of vacuolar acidification-induced transcription of genes of pathogens inside macrophages. *Mol Biol Cell* **17:** 498–510.

Mattheyses, A.L., Hoppe, A.D., and Axelrod, D. (2004) Polarized fluorescence resonance energy transfer microscopy. *Biophys J* **87:** 2787–2797.

Meresse, S., Steele-Mortimer, O., Moreno, E., Desjardins, M., Finlay, B., and Gorvel, J.-P. (1999) Controlling the maturation of pathogen-containing vacuoles: a matter of life and death. *Nature Cell Biol* **1:** E183–E188.

Miesenbock, G., De Angelis, D.A., and Rothman, J.E. (1998) Visualizing secretion and synaptic transmission with pH-sensitive green fluorescent proteins. *Nature* **394:** 192–195.

Nadrigny, F., Rivals, I., Hirrlinger, P.G., Koulakoff, A., Personnaz, L., Vernet, M., *et al.* (2006) Detecting fluorescent protein expression and co-localisation on single secretory vesicles with linear spectral unmixing. *Eur Biophys J* **35:** 533–547.

Neher, R., and Neher, E. (2004) Optimizing imaging parameters for the separation of multiple labels in a fluorescence image. *J Microsc* **213:** 46–62.

Nguyen, A.W., and Daugherty, P.S. (2005) Evolutionary optimization of fluorescent proteins for intracellular FRET. *Nat Biotechnol* **23:** 355–360.

O'Connor, N., and Silver, R.B. (2007) Ratio imaging: practical considerations for measuring intracellular Ca2+ and pH in living cells. *Meth Cell Biol* **81:** 415–433.

Oheim, M., and Dongdong, L. (2007) Quantitative colocalization imaging: concepts, measurements and pitfalls. In *Imaging Cellular and Molecular Biological Functions*. Shorte, S.L., and Frischknecht, F. (eds). Springer: Berlin, pp. 117–155.

Patterson, G.H., and Lippincott-Schwartz, J. (2002) A photoactivatable GFP for selective photolabeling of proteins and cells. *Science* **297:** 1873–1877.

Pawley, J.B. (2006) *Handbook of Biological Confocal Microscopy*. New York: Springer.

Piwnica-Worms, D., Schuster, D.P., and Garbow, J.R. (2004) Molecular imaging of host–pathogen interactions in intact small animals. *Cell Microbiol* **6:** 319–331.

Rajashekar, R., Liebl, D., Seitz, A., and Hensel, M. (2008) Dynamic remodeling of the endosomal system during formation of salmonella-induced filaments by intracellular *Salmonella enterica*. *Traffic* **9:** 2100–2116.

Roberts, E.A., Chua, J., Kyei, G.B., and Deretic, V. (2006) Higher order Rab programming in phagolysosome biogenesis. *J Cell Biol* **174:** 923–929.

Rust, M.J., Bates, M., and Zhuang, X. (2006) Sub-diffraction-limit imaging by stochastic optical reconstruction microscopy (STORM). *Nat Methods* **3:** 793–795.

Schermelleh, L., Carlton, P.M., Haase, S., Shao, L., Winoto, L., Kner, P., *et al.* (2008) Subdiffraction multicolor imaging of the nuclear periphery with 3D structured illumination microscopy. *Science* **320:** 1332–1336.

Sekar, R.B., and Periasamy, A. (2003) Fluorescence resonance energy transfer (FRET) microscopy imaging of live cell protein localizations. *J Cell Biol* **160:** 629–633.

Seveau, S., Bierne, H., Giroux, S., Prevost, M.C., and Cossart, P. (2004) Role of lipid rafts in E-cadherin- and HGF-R/Met-mediated entry of *Listeria monocytogenes* into host cells. *J Cell Biol* **166:** 743–753.

Seveau, S., Tham, T.N., Payrastre, B., Hoppe, A.D., Swanson, J.A., and Cossart, P. (2007) A FRET analysis to unravel the role of cholesterol in Rac1 and PI 3-kinase activation in the InlB/Met signalling pathway. *Cell Microbiol* **9:** 790–803.

Shaner, N., Campbell, R., Steinbach, P., Giepmans, B., Palmer, A., and Tsien, R. (2004) Improved monomeric red, orange and yellow fluorescent proteins derived from *Discosoma* sp. red fluorescent protein. *Nat Biotechnol* **22:** 1567–1572.

Shaughnessy, L.M., Hoppe, A.D., Christensen, K.A., and Swanson, J.A. (2006) Membrane perforations inhibit lysosome fusion by altering pH and calcium in *Listeria monocytogenes* vacuoles. *Cell Microbiol* **8:** 781–792.

Shroff, H., Galbraith, C.G., Galbraith, J.A., and Betzig, E. (2008) Live-cell photoactivated localization microscopy of nanoscale adhesion dynamics. *Nat Methods* **5:** 417–423.

Simpson, A.W. (2006) Fluorescent measurement of [Ca2+]c: basic practical considerations. *Methods Mol Biol* **312:** 3–36.

Veiga, E., Guttman, J.A., Bonazzi, M., Boucrot, E., Toledo-

Arana, A., Lin, A.E., *et al.* (2007) Invasive and adherent bacterial pathogens co-Opt host clathrin for infection. *Cell Host Microbe* **2:** 340–351.

Verveer, P.J., and Jovin, T.M. (1997) Efficient superresolution restoration algorithms using maximum *a posteriori* estimations with application to fluorescence microscopy. *J Opt Soc Am A* **14:** 1696.

Viboud, G.I., and Bliska, J.B. (2005) Yersinia outer proteins: role in modulation of host cell signaling responses and pathogenesis. *Annu Rev Microbiol* **59:** 69–89.

Wong, K.W., and Isberg, R.R. (2005) Yersinia pseudotuberculosis spatially controls activation and misregulation of host cell Rac1. *PLoS Pathog* **1:** e16.

Yeung, T., Touret, N., and Grinstein, S. (2005) Quantitative fluorescence microscopy to probe intracellular microenvironments. *Curr Opin Microbiol* **8:** 350–358.